Effect of Grain Boundary on Pseudo-elastic Deformation of Cu-Zn-Si Bicrystal of Shape Memory Alloy

AUTHOR(S):

MIURA, Sei; HAMASHIMA, Kazuo; HASHIMOTO, Satoshi; NAKANISHI, Norihiko

CITATION:

MIURA, Sei ...[et al]. Effect of Grain Boundary on Pseudo-elastic Deformation of Cu-Zn-Si Bicrystal of Shape Memory Alloy. Memoirs of the Faculty of Engineering, Kyoto University 1985, 47(2): 101-113

ISSUE DATE:

1985-07-15

URL:

http://hdl.handle.net/2433/281292

Effect of Grain Boundary on Pseudo-elastic Deformation of Cu-Zn-Si Bicrystal of Shape Memory Alloy

By

Sei MIURA*, Kazuo HAMASHIMA**, Satoshi HASHIMOTO*
and Norihiko NAKANISHI***

(Received November 28, 1984)

Synopsis

Two sorts of Cu-Zn-Si pseudo-elastic bicrystals of shape memory alloy were tested in tension to know the effects of the grain boundary. The remaining martensites were observed in the vicinity of the grain boundary, and the propriety of analyses through use of m/m_o and N_{ij} values and of the compatibility of the plastic strain were studied.

The variant of martensite occurring primarily in each grain during deformation, can be predicted with use of them value (shear factor of the variant) in general.

The analyses through use of m/m_i and N_{ij} values and the equations of the plastic strain compatibility are sufficiently useful to know the variant of martensite nucleated additionally in the vicinity of the grain boundary. However, the possibility of activation of slip must be considered in this case.

The reversible strain of the isoaxial bicrystal is larger than that of the non-isoaxial bicrystal. However, the relation between the reversible strain and the misorientation of bicrystal is not yet sufficiently known.

1. Introduction

The pseudo-elasticity and the shape memory effect have recently received much attention. These phenomena are specific to alloys transformed by the thermo-elastic martensite, and have been corroborated with Au-Cd,[1)-5)] Ni-Ti,[6)] Ag-Cd,[7)8)] Cu-Zn-X (X=Si, Sn, Al) ,[9)-12)] Cu-Sn,[13)14)] Cu-Al-Ni[15)] etc. Many workers studied these alloys, and clarified that these phenomena are obtained successfully on a single crystal, but are not obtained sufficiently on most polycrystals, except for the polycrystal of Ni-Ti which is an aggregate of extremely fine grains.

* Department of Engineering Science, Faculty of Engineeing, Kyoto University, Kyoto, Japan.
** Department of Mechanical Engineeing, Doshisha University, Kyoto, Japan.
*** Deparment of Chemistry, Faculty of Science, Konan University, Kobe, Japan.

The extinction of these phenomena on polycrystal is primarily caused by the effect of the grain boundary, such as the occurrence of a boundary crack. These effects are considered to be due to the obstruction of the reverse transformation of martensite, formed in the vicinity of the grain boundary, by the grain boundary. Therefore, to study these effects is significant. However, an investigation using polycrystal does not sufficiently satisfy the intention, because the effects of the grain boundaries are duplicated complicatedly. Finally, an investigation using bicrystal, having only a grain boundary, is most useful. Such an attempt, in spite of the usefulness, has been performed scarcely at all, save for the work of Takezawa et al. ,[16] using Cu-Zn-Al alloy bicrystals.

On the other hand, the effects of the grain boundary on normal plastic deformation by slips have been investigated variously by many investigators, using bicrystals of Al,[17)-21)] Fe-Si[22)] etc. As a result of these investigations, it was determined that the effects are due to additional slips in the vicinity of the grain boundary, and to the back-stress caused by the piled-up dislocations against the grain boundary. Some additional slips are induced by slips of an adjacent grain, and some are activated to satisfy the compatibility of the elastic or plastic strain at a grain boundary plane. Subsequently, the geometrical analyses on induced slips and the strain compatibility have been established.

In this study, Cu-Zn-Si alloy bicrystals were stretched several times by various strains until producing a permanent strain, to clarify fundamentally the effects of the grain boundary on the pseudo-elastic phenomenon. An application of the geometrical analyses estabrished in deformation by slips to the martensitic deformation is attempted subsequently.

2. Experimental procedure

2. 1 Preparation of specimens

The material used in this investigation was a rolled material having chemical compositions of Cu-36. 8at%Zn-1. 0at%Si. Bicrystal plates were grown in argon atmosphere by the Bridgman method, and homogenized by annealing at 1083K for 5hr. Bicrystal specimens were cut from the plates by spark cutting, and polished mechanically and electrolytically. The specimens, confined in quartz tubes under a partical pressure of argon, were solutions treated at 1123K for 30 min. and then quenched into ice-brine to retain the β-phase. All specimens were polished mechanically and electrolytically before the tensile tests. Forthermore, the bicrystal specimen had a gauge dimension of 0. 8㎜×4㎜×12㎜, and a grain boundary in the central section and parallel to the tensile direction in subsequent tensile testing.

2.2 Features of bicrystal specimen and tensile test

The orientations of bicrystals used in this experiment are shown in Fig. 1 (a) (b) . In this paper, the bicrystals shown in Fig. 1 (a) (b) , are termed #25 bicrystal and #11 bicrystal respectively. The #25 bicrystal is a non-isoaxial bicrystal obviously, but both of the component grains of the #11 bicrystal have almost the same tensile orientations, i. e. this bicrystal can be regarded as an isoaxial bicrystal. The determination of the orientation was made by the back-Laue X-ray reflection method with an accuracy within $\pm$ 1°.

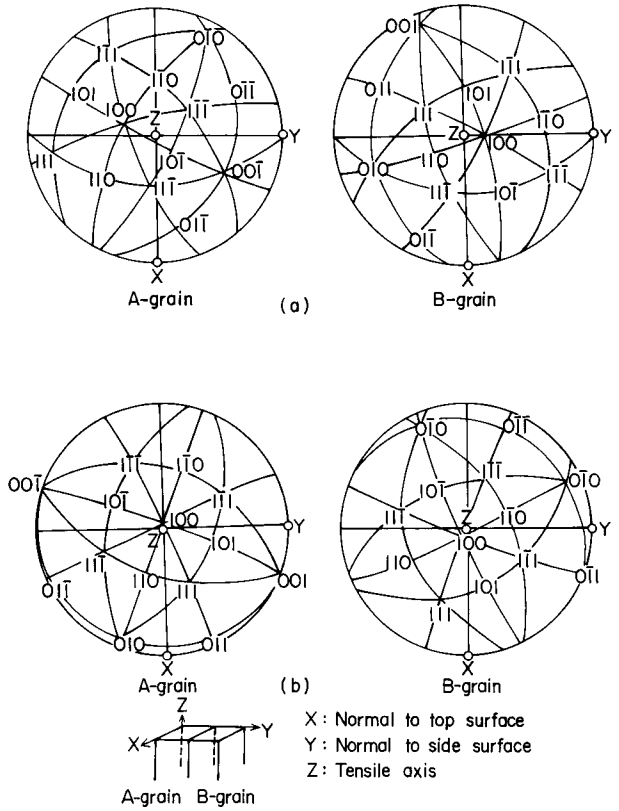

Fig. 1 Stereographic projections of bicrystals termed (a) the #25 bicrystal and (b) the #11 bicrystal.

The relations between the electric resistance and temperature in the cooling of both bicrystal specimens were also examined. Then, the starting and finishing temperatures (M_s and M_f) on the martensitic transformation of both bicrystals were determined from these relations. Finally, M_s and M_f of the #25 bicrystal were 233K and 206K, and those of the #11 bicrystal were 158K and 140K respectively.

The tensile tests were carried out with a strain rate of 2.78×10^{-4} sec^{-1} by using

an Instron type testing machine. The deformation temperatures of 263K and 203K were taken for the #25 bicrystal and for the #11 bicrystal respectively. After giving a proper strain to the specimen, the load was removed, and surface observations were made on the top surface of the specimen.

3. Results and discussion

3.1 Non-isoaxial bicrystal (#25 bicrystal)

3.1.1. Results of tensile test

Figure 2 (a) - (d) show the stress-strain curves of the #25 bicrystal stretched by about 3, 5, 10 and 15% strains respectively, and unloaded. At the deformation by 3%, a perfect pseudo-elastisity is produced and no permanent deformation (set) remains, but the permanent strain of only about 0.1% is obtained at the deformation by 5%. Furthermore, the permanent strains of 0.5% and 4% remain respectively at the deformations by 10% and 15%. Pops[10] exhibited the pseudo-elastic stress-strain curve of the Cu-34.1 at% Zn-1.8at%Si single crystal tested in compressin, and its

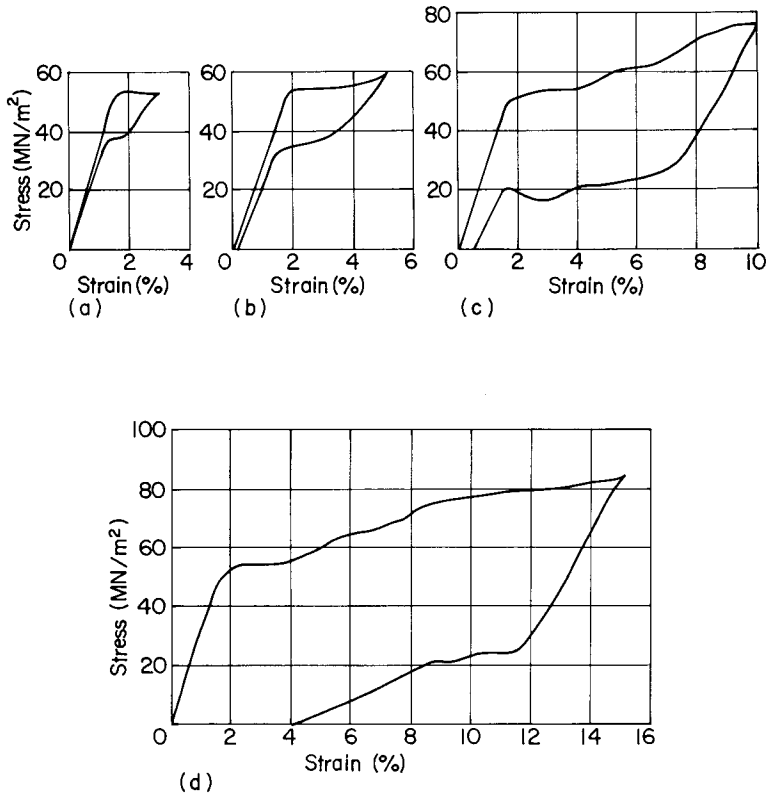

Fig. 2 Stress-strain curves of the #25 bicrystal streted by (a) 3.0% strain, (b) 5.0% strain, (c) 10.0% strain and (b) 15.0% strain.

peculiarlty has a good agreement with that of the curves obtained in the present invetigation.

No martensite plate was observed in the gauge section of the unloaded bicrystal after the deformation by 5% in spite of the permanent set at the stress-strain curve.

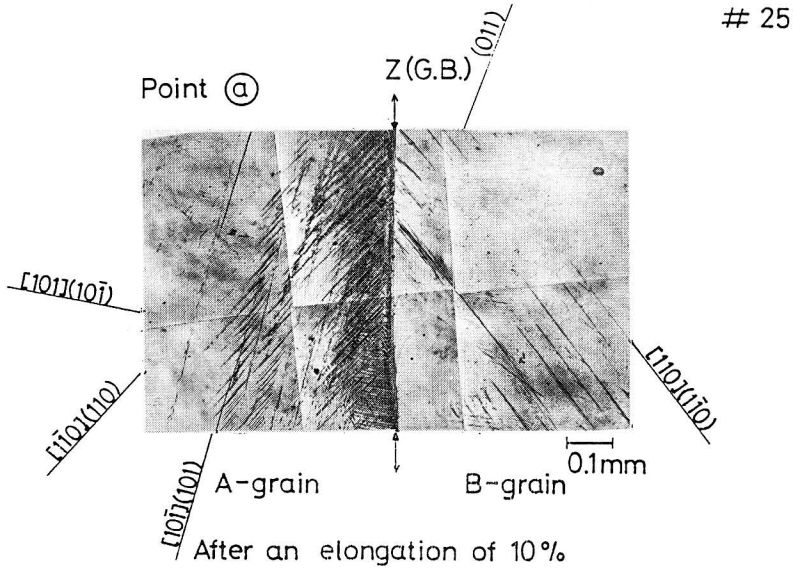

Fig. 3 Surface observation in the #25 bicrystal after an elongation of 10.0%.

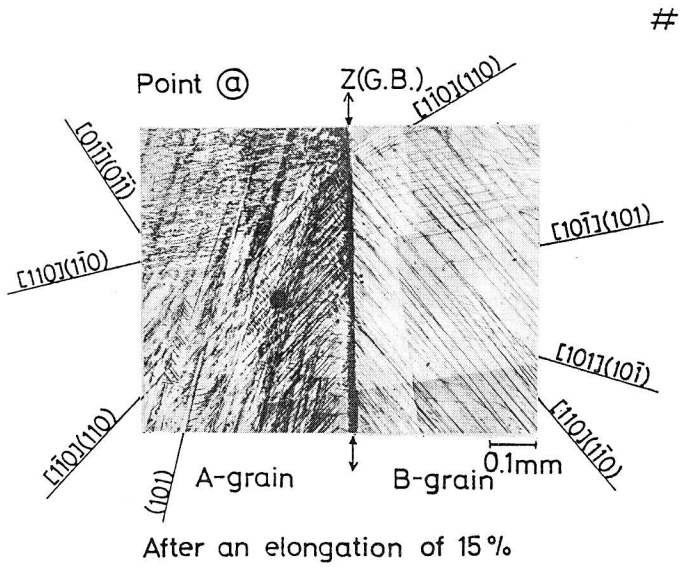

Fig. 4 Surface observation obtained in the #25 bicrystal after an elongation of 15.0%.

However, the grain boundary of this bicrystal has a sharp crook and a branch at the end of the bicrystal, and many martensite plates remain due to the complex stress distribution in these points. Therefore, it is concluded that the permanent set after the deformation by 5% is caused by the remaining martensites at these points.

Photographs taken from the observation surface of the bicrystal, polished slightly and etched electrolytically after the deformations by 10% and 15%, are given in Figs. 3 and 4 respectively. The habit plane of the martensite in Cu-Zn based β-phase alloy is {2, 11, 12} exactly[9], but is regarded as {110} in the present work for the convenience of later analyses, i. e. the deformation system by martensites is assumed to be the shear system on {110} 〈110〉. The index of the assumed shear system (variant) of the martensite plate is shown in the photographs.

After the deformation by 10%, the deformation plates of $(10\bar{1})$ $[101]$ and (110) $[1\bar{1}0]$ variants remain in the A-grain side of the grain boundary, and those of the $(1\bar{1}0)$ $[110]$ variants remain in its B-grain side Fig. 3. Furthermore, fine marks on the (011) trace are observed in the vicinity of the grain boundary in the B-grain. Figure 4 shows that martensite plates of various variants remain in both grains, and notched lines appear in the B-grain side of the grain boundary after the deformation by 15%. These photographs clarify that the variants of martensites introduced primarily during the deformation (primary variant) in each grain are (110) $[1\bar{1}0]$ in the A-grain and $(1\bar{1}0)$ $[110]$ in the B-grain.

3. 1. 2 Analysis of martensite plates remaining in the vicinity of the grain boundary

Livingston and Chalmers[18] reported that the slip system of additional slips in the vicinity of the grain boundary could be predicted with use of the stress transmission factor : N_{ij} value, using aluminum bicrystals. Saeki and Miura[20], subsequently maintained that the prediction became more exact by consideration of the ratio of the Schmid factor : m/m_o. Also, it is well known that additional slips in the vicinity of the grain boundary occur to satisfy the compatibility of the plastic strain at the grain boundary plane in general.

In this paper, the determination of variants of remaining matensite plates in the vicinity of the grain boundary is attempted with use of the N_{ij} value and m/m_o value and the compatibility of the plastic strain at the grain boundary plane. However, the shear system of the martensite plate is assumed to be {110} 〈110〉.

The values of m, m/m_o and N_{ij} for each variant in the A-grain due to the primary variant: $(1\bar{1}0)$ $[110]$ in the B-grain or for each variant in the B-grain due to the primary variant: (110) $[1\bar{1}0]$ in the A-grain, are given in Table 1. The value of m is the coefficient of the shear stress for a variant in a grain, and the m/m_o value is the ratio of the m value for each variant to maximum m value : m_o in the grain. In Table

Table 1 The value of m, m/mo and N_{ij} against each variant of A-grain due to the primary variant: $(1\bar{1}0)$ [110] of B-grain or against each variant of B-grain due to the primary variant: (110) $[1\bar{1}0]$ of A-grain, in the #25 bicrystal.

grain	variant	m	m/m_o	N_{ij}
A	$(101)\ [10\bar{1}]$ $(10\bar{1})\ [101]$	0.312	0.855	0.587
	$(01\bar{1})\ [0\bar{1}\bar{1}]$ $(0\bar{1}\bar{1})\ [01\bar{1}]$	0.089	0.244	0.322
	$(110)\ [1\bar{1}0]$ $(1\bar{1}0)\ [110]$	0.365	1	0.249
B	$(10\bar{1})\ [101]$ $(101)\ [10\bar{1}]$	0.405	0.985	0.417
	$(011)\ [01\bar{1}]$ $(01\bar{1})\ [011]$	0.031	0.075	0.153
	$(110)\ [1\bar{1}0]$ $(1\bar{1}0)\ [110]$	0.411	1	0.249

Table 2 Plastic strain components of all varlant and a slip system in the #25 bicrystal.

grain	variant	ε_{xx}	ε_{yy}	ε_{zz}
A	$(101)\ [10\bar{1}]$ $(10\bar{1})\ [101]$	0.312	−0.090	−0.307
	$(01\bar{1})\ [0\bar{1}\bar{1}]$ $(0\bar{1}\bar{1})\ [01\bar{1}]$	0.089	0.285	0.348
	$(1\bar{1}0)\ [110]$ $(110)\ [1\bar{1}0]$	0.365	−0.385	−0.051
B	$(101)\ [10\bar{1}]$ $(10\bar{1})\ [101]$	0.405	−0.517	0.127
	$(011)\ [01\bar{1}]$ $(01\bar{1})\ [011]$	0.031	−0.418	0.212
	$(110)\ [1\bar{1}0]$ $(1\bar{1}0)\ [110]$	0.411	−0.050	−0.069
	$(011)\ [11\bar{1}]$	0.198	−0.111	−0.111

2, three components of plastic strain for each variant in both grains are tabulated.

As the $(1\bar{1}0)$ [110] variant in the B-grain has the maximum m value in both grains, the martensite on this variant occurs at first. The additional stress by this martensite induces the martensite on the $(10\bar{1})$ [101] variant, having a large m/m_o value (0.855) and a relative large N_{ij} value (0.587), in the A-grain side of the grain boundary. Therefore in the A-grain, the martensite on the $(10\bar{1})$ [101] variant interacts with the martensite on the primary variant: (110) $[1\bar{1}0]$ in the vicinity of the grain boundary, and the reverse-transformation of martensites on both variants are obstructed. It can not be thought that the fine marks observed in Fig. 3 correspond with martensites induced by the martensites on the primary variant: $(110)\ [1\bar{1}0)$ of A-grain.

The sums of three components of plastic strain for the martensites which

occurred in the vicinity of the grain boundary, are $\varepsilon_{xx} = -0.475$, $\varepsilon_{zz} = 0.677$, $\varepsilon_{xz} = -0.358$ in the A-grain ((101) [10$\bar{1}$] and (110) [1$\bar{1}$0]) , and are $\varepsilon_{xx} = -0.050$, $\varepsilon_{zz} = 0.411$, $\varepsilon_{xz} = -0.069$ in the B-grain (only (1$\bar{1}$0) [110]) . The difference between both grains are ($\Delta\varepsilon_{xx} = 0.425$, $\Delta\varepsilon_{zz} = 0.266$, $\Delta\varepsilon_{xz} = 0.289$, and the im-

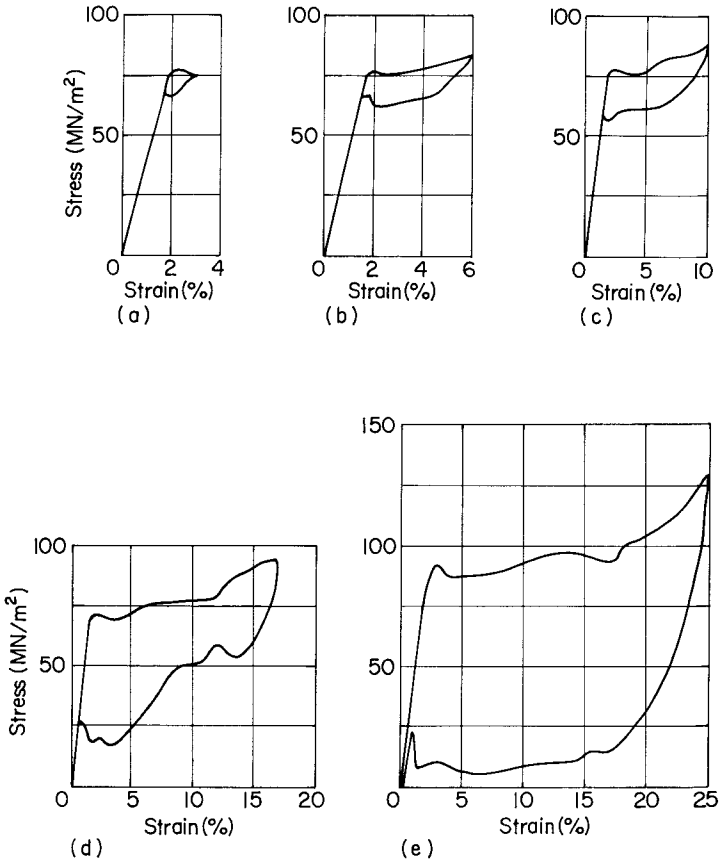

Fig. 5 Stress-strain curves of the #11 11 bicrystal stretched by (a) 3.0% strain, (b) 6.0% strain, (c) 10.0% strain, (d) 17.0% strain and (e) 25.0% strain.

compatibility is remarkable. The imcompatibility is not decreased by the addition of a martensite on (011) [01$\bar{1}$] ($\Delta\varepsilon_{xx} = 0.235$, $\Delta\varepsilon_{zz} = 0.007$, $\Delta\varepsilon_{xz} = 0.501$) , but is fairly decreased by the addition of slip on the (011) [11$\bar{1}$] system, the common slip system of Cu-Zn based β-phase alloy ($\Delta\varepsilon_{xx} = 0.068$, $\Delta\varepsilon_{zz} = 0.060$, $\Delta\varepsilon_{xz} = 0.178$) . The morphology of the fine mark observed in Fig. 3 is different from that of the martensite plate. It is concluded that these fine marks correspond with the (011) [11$\bar{1}$] slip which occurred to satisfy the compatibility of the plastic strain. However, the other slip is accompanied by a cross slip in the A-grain side of the grain

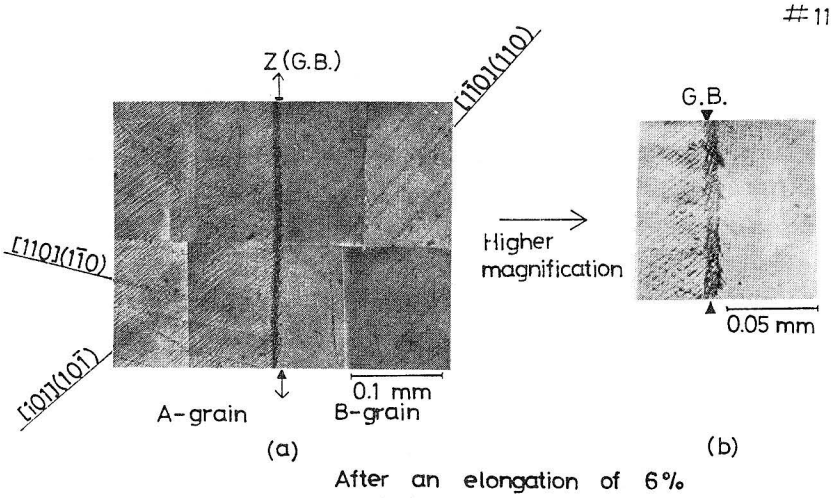

Fig. 6 Surface observation obtained in the #11 bicrystal after an elongation of 6.0%.

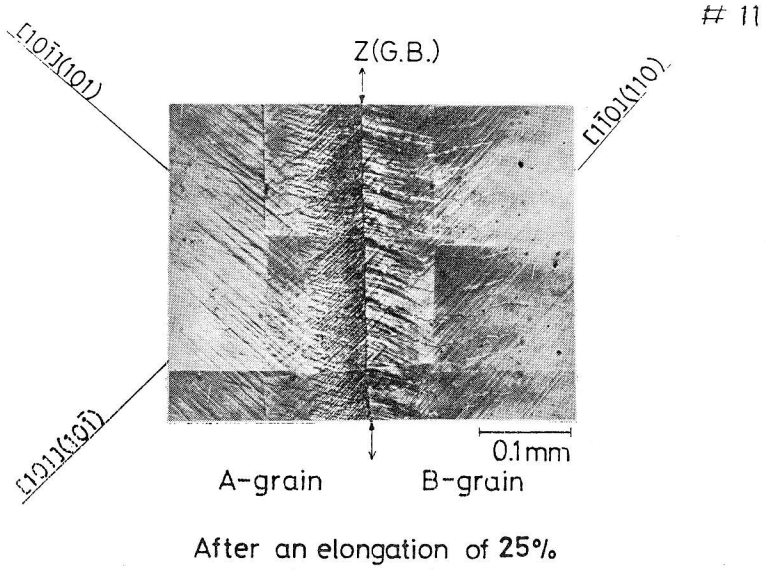

Fig. 7 Surface observation obtained in the #11 bicrystal after an elongation of 25.0%.

biundary because of the remaining imcompatibility at the deformation by a larger strain (Fig. 4) .

3. 2 Isoaxial bicrystal (#11 bicrystal)

3. 2. 1 Results of tensile test

Figure 5 (a) - (e) shows the stress-strain curves of the #11 bicrystal stretched by about 3%, 6%, 10%, 17% and 25% strains respectively, and unloaded. In this bicrystal, the whole applied elongation can be recovered pseudo-elastically at the deformations by 3%, 6%, 10% and 17% strains, and a permanent set (about 0. 3% strain) is obtained only at the deformation by a 25% strain. These curves have the same peculiarity as that of #25 bicrystal, but their winding points are sharper. The difference is thought to be due to the difference of the deformation temperature.

Figure 6 is the photograph taken from the top surface of this bicrystal after elongation by 6%. The traces of martensites on the $(10\bar{1})$ [101] and $(1\bar{1}0)$ [110] variants and the (110) $[1\bar{1}0]$ variant are observed in the A-grain and B-grain respectively, but no remaining martensite plane is observed in this photograph. However, observation with a higher magnification clarified that very short martensite plates on various variants remain touching the grain boundary. After the deformation by 25%, many martensite plates and slip lines, i. e. martensite plates on the $(10\bar{1})$ [101] variant and slip lines in the A-grain, and martensite plates on the (110) $[1\bar{1}0]$ variant and slip lines in the B-grain, are observed in the vicinity of the grain boundary (Fig. 7) . These results suggest that the primary variants of the A-grain and B-grain are $(10\bar{1})$ [101] and (110) $[1\bar{1}0]$ respectively.

3. 2. 2 Analysis of martensite plates remaining in the vicinity of the grain boundary

Analyses with use of the m/m_o value and N_{ij} value, and the compatibility of the plastic strain are attempted still with regard to the #11 bicrystal. The varues of m, m/m_o and N_{ij} for each variant in the A-grain due to the primary variant: (110) $[1\bar{1}0]$ in the B-grain or for each variant in the B-grain due to the primary variant: (101) $[10\bar{1}]$ in the A-grain, are given in Table 3. Subsequently, three components of the plastic strain for each variant in both grains are tabulated in Table 4.

As this bicrystal was cut from the as-grown bicrystal plate not homogenized, the solute atoms and so on have been segregated to the grain boundary. Therefore, the internal stress has been stored due to the segregation in the vicinity of the grain boundary. Since martensites on plural variants occur in the internal stress field even at a deformation by such a small strain, short martensite plates' remain touching the grain boundary after unloading (Fig. 6) .

To induce martensites additionally is fairly difficult at the deformation by a small strain in the #11 bicrystal, because martensites on the primary variant are introduced almost simultaneously in both grains. However, at the deformation by a large strain, the martensite on the $(10\bar{1})$ [101] variant having large m/m_o and N_{ij}

Table 3 The value of m, m/mo and Nij against each variant of A-grain due to the primary variant: $(1\bar{1}0)$ [110] of B-grain or each variant of B-grain due to the primary variant: $(10\bar{1})$ [101] of A-grain in the #11 bicrystal.

grain	variant	m	m/m_o	N_{ij}
A	(101) $[10\bar{1}]$ $(10\bar{1})$ $[101]$	0.491	1	0.682
	(110) $[1\bar{1}0]$ $(1\bar{1}0)$ $[110]$	0.475	0.967	0.645
	(011) $[01\bar{1}]$ $(01\bar{1})$ $[011]$	0.004	0.008	0.027
B	(101) $[10\bar{1}]$ $(10\bar{1})$ $[101]$	0.484	1	0.743
	(110) $[1\bar{1}0]$ $(1\bar{1}0)$ $[110]$	0.480	0.992	0.685
	$(0\bar{1}1)$ $[0\bar{1}\bar{1}]$ $(0\bar{1}\bar{1})$ $[0\bar{1}1]$	0	0	0.035

Table. 4 Plastic strain compoments of all varlants in the #11 bicrystal.

grain	variant	ε_{xx}	ε_{zz}	ε_{xz}
A	(101) $[10\bar{1}]$ $(10\bar{1})$ $[101]$	0.491	−0.056	−0.071
	(110) $[1\bar{1}0]$ $(1\bar{1}0)$ $[110]$	0.475	−0.433	−0.164
	(011) $[01\bar{1}]$ $(01\bar{1})$ $[011]$	0.004	0.360	0.087
B	(101) $[10\bar{1}]$ $(10\bar{1})$ $[101]$	0.484	−0.398	0.209
	(110) $[1\bar{1}0]$ $(1\bar{1}0)$ $[110]$	0.480	−0.075	0.191
	$(0\bar{1}1)$ $[0\bar{1}\bar{1}]$ $(0\bar{1}\bar{1})$ $[0\bar{1}1]$	0	−0.317	0.053

values (1 and 0.682) is induced at the A-grain side of the grain boundary by the martensite on the primary variant: $(1\bar{1}0)$ $1\bar{1}0]$ of the B-grain. Therefore, the interaction between martensites on the $(10\bar{1})$ [101] variant and the (101) $[10\bar{1}]$ variant takes place and the martensite plates on both variants remain in the vicinity of the grain boundary (Fig. 7) . In a case where the martensites nucleate on only the primary variants of both grains, the incompaticility of the plastic strain at the grain boundary is relatively small ($\Delta\varepsilon_{xx}$ =0.019, $\Delta\varepsilon_{zz}$ =0.011, $\Delta\varepsilon_{xz}$ =0.262). As the incompaticility is increased by the addition of induced martensites, the slip accompanied by a cross slip occurs at both sides of the grain boundary.

The maximum reversible strain of the #11 bicrystal (24% strain) is larger than that of the #25 bicrystal (10% strain). This difference is mainly caused by the

orientation dependence of the pseudo-elasticity and the different deformation temperatures. However it is thought that the relation between the orientations of both grains composing a bicrystal, and the easiness for nucleation of additional martensites are factors for determining the maximum reversible strain value.

4. Conclusion

Two sorts of Cu-Zn-Si pseudo-elastic bicrystals were tested in tension to know the effects of the grain boundary. The remaining martensites were observed in the vicinity of the grain boundary, and the propriety of analyses with use of the m/m_o and N_{ij} values and of the compatibility of the plastic strain were studied.

The variant of any martensite occurring primarily in each grain during deformation, can be predicted with use of the m value (shear factor of the variant) in general.

The analyses with use of the m/m_o and N_{ij} values and the equations of the plastic strain compatibility are sufficiently useful to know the variant of martensite nucleated additionally in the vicinity of the grain boundary. However, the possibility of activation of slip must be considered in this case.

The reversible strain of the isoaxial bicrystal (#11 bicrystal) is larger than that of the non-isoaxial bicrystal (#25 bicrystal). Since the relation between the reversible strain and the misorientation of the bicrystal is not yet sufficiently known, further investigations and discussions are expected.

References

1) D. S. Lieberman, M. S. Wechsler and T. A. Read, J. Appl. phys., **26**, 473 (1955) .
2) H. K. Birnbaum and T. A. Read, Trans. AIME, **218**, 662 (1960) .
3) N. Nakanishi and C. M. Wayman, Trans. AIME, **227**, 500 (1963)
4) N. Nakanishi, T. Mori, S. Miura, Y. Murakami and S. Kachi, Phil. Mag., **28**, 277 (1973) .
5) S. Miura, T. Mori and N. Nakanishi, "Mechanical Behavior of Materials" (Proc. 1974 Symp. of Mech. Behavior of Materials. Kyoto, 1974, The Society of Materials Science, Japan) , Vol. I I p. 141 (1974).
6) W. J. Bocher, J. V. Gilfrich and R. C. Wiley, J. Appl. Phys., **34**, 1475 (1963) .
7) R. V. Krishnan and L. C. Brown, Met. Trans., **4**, 432 (1973).
8) S. Miura, T. Mori and N. Nakanishi, Scripta Met., **7**, 697 (1973).
9) H. Pops, Trans. AIME, **239**, 756 (1967).
10) H. Pops, Met. Trans., **1**, 251 (1970).
11) J. D. Eisenwasser and L. C. Brown, Met. Trans., **3**, 1359 (1972).
12) D. V. Wieid and E. Gillam, Acta Met., **25**, 725 (1977).
13) S. Miura, S. Maeda and N. Nakanishi, Scripta Met., **9**, 675 (1975).
14) S. Miura, Y. Morita and N. Nakanishi, Proc. Int. Symposium on Shape Memory Effects and Applications, Toronto, p. 389 (1975).
15) K. Otsuka and K. Shimizu, Scripta Met., **4**, 469 (1970).
16) K. Takezawa, T. Izumi and S. Sato, Preprint of the 86th Meeting of Japan Inst. of Metal,

Tokyo, p. 44 (1980).
17) R. Clark and B. Chalmers, Acta Met., **2**, 80 (1954) .
18) J. D. Livingston and B. Chalmers, Acta Met., **5**, 322 (1957).
19) T. Inoko, K. Akizono and G. Mima, J. Japan Inst. Metals, **36**, 373, 380 (1972).
20) Y. Saeki and S. Miura, "Mechanical Behavior of Materials" (Proc. 1974 Symp. of Mech. Behavior of Materials. Kyoto, 1974. The Society of Materials Science, Japan) , Vol. I I p. 11 (1974).
21) O. Izumi and T. Takasugi, Z. Metallk., **65**, 542 (1974).
22) R. E. Hook and J. P. Hirth, Acta Met., **15** 535, 1099 (1967).